

Generic regimes of quantum many-body dynamics of trapped bosonic systems with strong repulsive interactions

Oksana I. Streltsova,¹ Ofir E. Alon,² Lorenz S. Cederbaum,³ and Alexej I. Streltsov³

¹Laboratory of Information Technologies, Joint Institute for Nuclear Research, Joliot-Curie 6, Dubna, Russia

²Department of Physics, University of Haifa at Oranim, Tivon 36006, Israel

³Theoretische Chemie, Physikalisch-Chemisches Institut, Universität Heidelberg, Im Neuenheimer Feld 229, D-69120 Heidelberg, Germany

(Received 13 December 2013; revised manuscript received 3 April 2014; published 27 June 2014)

The nonequilibrium quantum dynamics of trapped bosons interacting by strong interparticle interaction of finite range in one, two, and three spatial dimensions is investigated on an accurate many-body level. We use different time-dependent processes to destabilize the systems' ground states: A sudden quench of the strength of the interparticle repulsion is accompanied by displacement of the trap. Two qualitatively different but otherwise generic dynamical quantum many-body behaviors are discovered. In the first, the overall "topology" of the ground-state density is preserved, whereas in the second the density totally "explodes." An intuitive many-body time-dependent model is devised to interpret and explain the observations. The generality of the discovered scenarios is explicitly confirmed in traps of various shapes and dimensionality, and interparticle interactions of different forms and ranges. Implications are briefly discussed.

DOI: [10.1103/PhysRevA.89.061602](https://doi.org/10.1103/PhysRevA.89.061602)

PACS number(s): 03.75.Kk, 05.30.Jp, 03.65.-w, 67.85.-d

What are the fingerprints of strong interparticle interactions in trapped quantum systems? In the case of strong repulsive interactions the most relevant ones are formations of nontrivial structures in the ground states' densities and developments of strong correlations therein. These features are generic; namely they are shared by different many-body systems made of bosons and fermions, with various shapes and ranges of the repulsive interparticle interactions, and appear in different physical contexts. For example, the densities of the ground states are modulated in ultracold one-dimensional (1D) systems in the famous Tonks-Girardeau gas with short-range contact interaction [1,2], and in bosonic and fermionic systems with long-range Coulomb [3] interparticle interaction and its screened versions [4–7]. Examples in two dimensions (2D) are formations of supersolid and crystalline-like structures in dipolar and "Rydberg-dressed" systems with long- and finite-range repulsive interactions [8–14].

Static properties of trapped bosonic systems with finite- and long-range interaction have amply been studied in the literature at the full many-body level, for instance by means of quantum Monte Carlo techniques [3,8–12]. In contrast, much less is known on the nonequilibrium dynamics of these systems, especially in higher dimensions. In the context of dipolar and "Rydberg-dressed" ultracold bosonic systems, at which this work is primarily aimed, the quantum many-body dynamics has so far been addressed at the Gross-Pitaevskii (GP) mean-field level only [10,11,13,15–17]. Obviously, when the interaction gets stronger the many-boson systems can have properties and correlations in the ground state and more so in excitations which are not at all accessible within the GP description and full many-body solutions of the time-dependent Schrödinger equation (TDSE) are desirable.

The main objective of this Rapid Communication is to explore and understand the dynamical stability of bosonic systems with finite-range strong interactions as a time-dependent process on an accurate many-body level. For this, we solve the TDSE by applying the multiconfigurational time-dependent

Hartree for bosons (MCTDHB) method [18,19]; also see Refs. [20–27] for a few applications. The main results of this work are as follows: (i) We report on two qualitatively different but otherwise generic dynamical behaviors in the nonequilibrium dynamics of bosonic systems with finite-range strong interactions; (ii) we provide an intuitive many-body time-dependent model to interpret and explain the results; and (iii) we announce a breakthrough in quantum many-body nonequilibrium dynamics of trapped bosons in 2D and in 3D computed by the MCTDHB method.

As a preamble for the dynamics, we begin with a brief yet essential account of the system's ground state [14]. Consider a bosonic system with finite- or long-range repulsive interaction confined in a simple trap. By "simple" we mean a trap without a barrier. When the strength of the repulsion is increased, the ground-state density undergoes changes—the number of density maxima, hereafter referred to as density humps or just humps, increases. An illustrative example in 1D is shown in Fig. 1. In Ref. [14] it has been shown that the number of humps is governed by the geometrical interplay between the width of the interparticle interaction potential and the available volume (length of the trap) which depends on the strength of the repulsion. Equivalently, the ground state can be controlled by varying the tightness of the confinement or the number of trapped particles; for more information see Fig. S1 in the Supplemental Material [28] and Ref. [14].

At weak interaction the system is condensed (superfluid) and its ground-state density has a single maximum; see Fig. 1 and Fig. S1a in the Supplemental Material [28]. At stronger repulsion, the ground-state density develops additional density humps. Importantly, these changes in the ground-state density are accompanied by the loss of coherence between the density humps and the development of fragmentation. The fragmentation and condensation phenomena are rigorously defined via decomposition of the reduced one-particle density matrix [29–35] which is also used to quantify the coherence and correlations [36,37]. Generally, if the density has n humps the many-boson system is n -fold fragmented [14].

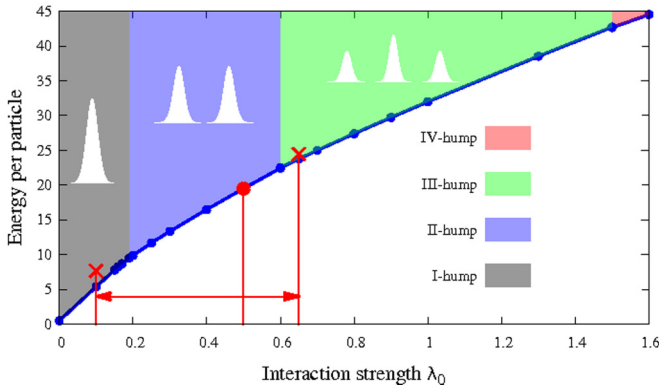


FIG. 1. (Color online) The ground state of interacting bosons confined in a 1D parabolic $V(x)=x^2/2$ trap becomes fragmented when the strength λ_0 of the finite-range interparticle repulsion is increased. The number of bosons is $N = 100$, the shape of interparticle interaction is $W(\mathbf{R})=1/[(|x-x'|/D)^n+1]$ with half width $D=4$ and $n=4$. The regions of λ_0 corresponding to one-, two-, three-, and four-hump densities are schematically shown. The big (red) dot depicts the initial state at $\lambda_0=0.5$ for the studied quench dynamics. The big (red) crosses indicate the energies of the evolving states induced by a sudden decrease $\lambda_0=0.5 \rightarrow 0.1$ and increase $\lambda_0=0.5 \rightarrow 0.65$ of the repulsion strength. See text for more details. All quantities shown are dimensionless.

In this Rapid Communication we study how stable these interaction-induced modulations of the ground states' densities are against external and internal disturbances in bosonic systems confined in 1D, 2D, and 3D setups. The stability is investigated as a time-dependent process by solving the real-space TDSE $\hat{H}\Psi = i\hbar\frac{\partial\Psi}{\partial t}$ for several dynamical scenarios involving manipulations with the external trap $V(\mathbf{r},t)$ and the strength λ_0 of inter-boson interaction potential $W(\mathbf{r}-\mathbf{r}') \equiv W(\mathbf{R})$. The respective many-body Hamiltonian is $\hat{H} = \sum_{j=1}^N [-\frac{1}{2}\nabla_{\mathbf{r}_j}^2 + V(\mathbf{r}_j,t)] + \sum_{j<k}^N \lambda_0 W(\mathbf{r}_j-\mathbf{r}_k)$, $\hbar=1$, $m=1$. All the results reported in this work have been obtained for $N = 100$ bosons interacting via interparticle interaction function $W(\mathbf{R})=1/[(|\mathbf{r}-\mathbf{r}'|/D)^n+1]$ of half width $D=4$ with $n=4$ in 1D, 2D, and 3D. Two-body interactions of similar shapes [38] naturally appear in the so-called ‘‘Rydberg-dressed’’ ultracold systems (see [39–41]) which are of current experimental interest [42]. The repulsive interparticle interactions of other shapes with similar range and strength would result in qualitatively the same physics.

Let us first investigate the dynamical stability of a two-hump twofold fragmented system in 1D, obtained as the ground state of $N = 100$ bosons with $\lambda_0=0.5$; see Fig. 1 and Fig. S1b in the Supplemental Material [28]. At $t=0$ we suddenly displace the trap $V(x) \rightarrow V(x-1)$. The computed density of the evolving many-body wave packet is depicted in Fig. 2(a). The main observation is that this manipulation of the trap does not change the overall ‘‘shape’’ of the density. We hereafter refer to such a scenario as a nonviolent dynamics. Furthermore, the twofold fragmentation of the system persists for all the presented times.

Now we enrich the dynamical scenario by imposing onto the same initial system at $t=0$ together with the sudden displacement of the trap also a sudden quench of the interparticle repulsion from $\lambda_0=0.5 \rightarrow 0.65$. With this

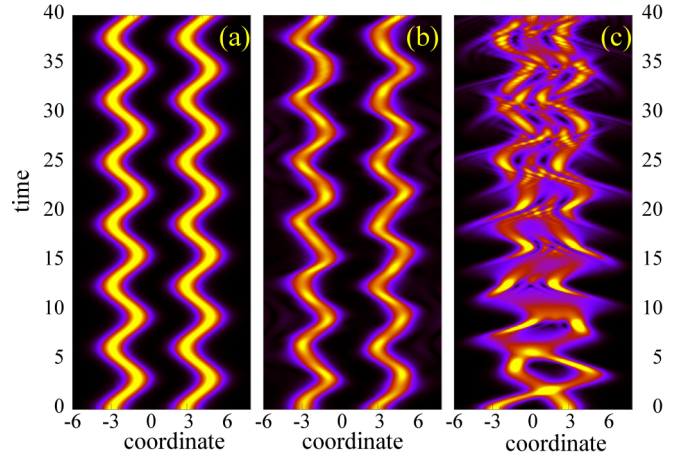


FIG. 2. (Color online) Two generic scenarios of many-body dynamics in 1D induced by a sudden displacement of the harmonic trap $V(x) \rightarrow V(x-1)$ and a simultaneous quench of the interparticle repulsion. The initial state is the twofold fragmented ground state of $N = 100$ bosons with $\lambda_0=0.5$. Evolutions of the density are plotted for the scenarios activated by the displacement of the trap (a) without quench of the repulsion, (b) with small increase of the repulsion $\lambda_0=0.5 \rightarrow 0.65$, and (c) with substantial decrease of the repulsion $\lambda_0=0.5 \rightarrow 0.1$. Panels (a) and (b) reveal the first generic regime: nonviolent (under-a-barrier) dynamics, in which the density preserves its ‘‘topology.’’ Panel (c) represents the second regime: highly nonequilibrium (over-a-barrier) dynamics, characterized by explosive changes of the density. All quantities shown are dimensionless.

quench of the interaction strength we bring the system into the regime where the ground state has a three-hump density; see Fig. 1. The time-dependent density depicted in Fig. 2(b) reveals along with a relative simple motion induced by the trap displacement additional features. The density humps change their widths during the evolution; i.e., they ‘‘breathe.’’ These breathings slightly disturb and modulate the perfect harmonic-like oscillations of the density.

Next, in a third scenario we take the same initial state as before, suddenly displace the trap at $t=0$, but now decrease the strength of the interparticle repulsion from $\lambda_0=0.5 \rightarrow 0.1$. At this value of the interparticle interaction the ground state of the final system has a single hump and is fully condensed; see Fig. 1 and Fig. S1a in the Supplemental Material [28]. Hence, this scenario can be considered as an attempt to make a superfluid from an initially fragmented system. The corresponding evolution of the density is shown in Fig. 2(c). The wave packet reveals highly nonequilibrium explosive dynamics which is accompanied by the formation of complicated oscillating patterns in the density. The character of this dynamics differs drastically from the evolutions studied above; compare panels (a) and (b) with panel (c) of Fig. 2.

Both scenarios with quenched interparticle interactions bring the initial many-body system to the regimes with different ‘‘topologies’’ of the ground states; see bold crosses in Fig. 1. So, from the perspective of the ground-state diagram one would naively expect a similar character of the dynamics in both cases. However, the studied 1D many-body systems demonstrate two qualitatively different reactions: a nonviolent and a highly nonequilibrium, explosive one. The first claim of

this Rapid Communication is that these reactions are generic features of disturbed strongly interacting repulsive fragmented systems.

To understand the physics behind the observed nonviolent and explosive many-body dynamics, we extend the concept of self-induced effective barriers introduced in Ref. [14] to explain the density humps in the ground state. Intuitively, one can associate each hump of the evolving multihump system with a well-isolated time-evolving fragment $\phi_k(\mathbf{r}, t)$. In the two-hump cases depicted in Figs. 2(a) and 2(b) one can assume that half of bosons $\frac{N}{2}$ are residing in the left evolving fragment $\phi_L(\mathbf{r}, t)$ and the other half in the right one $\phi_R(\mathbf{r}, t)$. The respective time-dependent permanent (symmetrized configuration) reads $\hat{S}\phi_L(\mathbf{r}_1, t) \cdots \phi_L(\mathbf{r}_{\frac{N}{2}}, t)\phi_R(\mathbf{r}_{\frac{N}{2}+1}, t) \cdots \phi_R(\mathbf{r}_N, t) \rightarrow |\frac{N}{2}, \frac{N}{2}, t\rangle$. For a realistic description this idealized picture of a single configuration with a fixed number of particles residing in each time-evolving fragment should be augmented by other processes describing, e.g., the exchange and hopping of particles between the fragments. In the MCTDHB method the many-body wave function is constructed as a linear combination of all possible *time-dependent* configurations obtained by permuting N bosons over M fragments $\Psi(\mathbf{r}_1, \dots, \mathbf{r}_N, t) = \sum_{\vec{n}} C_{\vec{n}}(t) |n_1, n_2, \dots, n_M, t\rangle$. The MCTDHB equations [18, 19],

$$i \frac{\partial \phi_j}{\partial t} = \hat{\mathbf{P}} \left[\hat{h} \phi_j(\mathbf{r}, t) + \lambda_0 \sum_{qksl} \{\rho(t)\}_{jq}^{-1} \rho_{qksl}(t) W_{kl}(\mathbf{r}, t) \phi_s(\mathbf{r}, t) \right],$$

$$i \frac{dC_{\vec{n}}}{dt} = \sum_{\vec{n}'} \langle \Phi_{\vec{n}} | \hat{H} | \Phi_{\vec{n}'} \rangle C_{\vec{n}'}(t) \quad (1)$$

[$\hat{h} = \hat{T}(\mathbf{r}) + V(\mathbf{r})$ is the single-particle Hamiltonian], describe changes of the shape of every fragment $\phi_j(\mathbf{r}, t)$ and the evolution of the coefficients $C_{\vec{n}}(t)$, i.e., all hopping processes in the system. During the propagation, each of the fragments “feels” the external trap potential and, also, time-dependent effective potential barriers $W_{kl}(\mathbf{r}, t) = \int \phi_k^*(\mathbf{r}', t) W(\mathbf{r} - \mathbf{r}') \phi_l(\mathbf{r}', t) d\mathbf{r}'$ induced by the other fragments as a result of the interparticle interaction. The intensities, i.e., heights of the induced barriers, are proportional to the strength λ_0 of the repulsion and to the

ratio $\{\rho(t)\}_{jq}^{-1} \rho_{qksl}(t)$ of the involved elements of two- and one-body density matrices. In the case of an ideal fragmented state with well-localized fragments, this ratio is proportional to the number of particles residing in each fragment. For instance, in a perfect twofold fragmented system it approaches $N/2$ and the overall potential seen by the left, right fragment, $\phi_k(\mathbf{r}, t)$, $k=L, R$, is the superposition of the external trap $V(\mathbf{r})$ and the effective time-dependent barrier $V_{jj}^{\text{eff}}(\mathbf{r}, t) = \lambda_0 \frac{N}{2} W_{jj}(\mathbf{r}, t) = \lambda_0 \frac{N}{2} \int |\phi_j(\mathbf{r}', t)|^2 W(\mathbf{r} - \mathbf{r}') d\mathbf{r}'$ induced by the counterpart fragment, $j=R, L$.

The second claim of this Rapid Communication is that the physics behind the two qualitatively different quantum many-body behaviors seen in Fig. 2 can be interpreted as under- and over-a-barrier dynamics. When the manipulations exerted on the system are not strong enough to destroy or overcome the induced time-dependent barriers $V_{jj}^{\text{eff}}(\mathbf{r}, t)$, the dynamics takes place under-a-barrier and the system behaves in the nonviolent manner discussed above. Otherwise, the dynamics occurs over-a-barrier and the system enters a regime with a highly nonequilibrium dynamics, characterized by violent explosive behavior of the density. Despite the intuitive physics behind this, the construction of a simple analytic model capable of predicting the over- or under-a-barrier regimes seems to be a challenging theoretical problem. This is because the details of the many-body system, e.g., shapes of the trapping and interaction potentials, number of particles, strength of the interaction, as well as the “direction” of the quench, are very crucial. Fortunately, modern computational physics makes the required full many-body propagation via MCTDHB Eqs. (1) feasible for the studied Hamiltonians, including also at higher dimensions.

We would now like to investigate the nonequilibrium dynamics of a strongly repulsive trapped Bose system in 2D. Our aim is to confirm and verify the generality of the above-found dynamical regimes also in higher dimensions. The many-body dynamics is induced by a sudden displacement of the 2D trap $V(x, y) = 0.5x^2 + 1.5y^2 \rightarrow V(x - 1.5, y - 0.5)$ with simultaneous quenches of the repulsion. The initial state is the two-hump ground state of $N = 100$ bosons trapped in $V(x, y)$ with $\lambda_0 = 0.5$. In the lower parts of Fig. 3 we

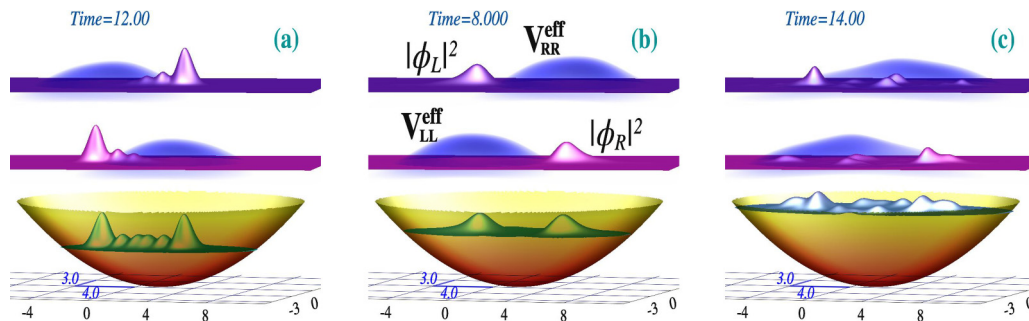


FIG. 3. (Color online) Visualization of the concept of interaction-induced time-dependent barriers to interpret the two generic dynamical regimes of strongly interacting trapped bosons: a 2D case. Evolutions of a twofold fragmented initial state induced by a sudden displacement of the harmonic trap $V(x, y) \rightarrow V(x - 1.5, y - 0.5)$ with a simultaneous quench of the interparticle repulsion: (a) strong decrease $\lambda_0 = 0.5 \rightarrow 0.1$, snapshot at $t = 12$; (b) moderate increase $\lambda_0 = 0.5 \rightarrow 0.7$, snapshot at $t = 8$; (c) stronger increase $\lambda_0 = 0.5 \rightarrow 0.8$, snapshot at $t = 14$. The density and trap are depicted on the lower parts. The upper parts show the density $|\phi_k(\mathbf{r}, t)|^2$ of the left (right) fragment and the time-dependent barriers $V_{jj}^{\text{eff}}(\mathbf{r}, t)$ induced by the complementary right (left) fragment. The over-a-barrier dynamics [(a), (c)] happens when the energy per particle of the out-of-equilibrium state is larger than the heights of the induced barriers; otherwise the dynamics is under-a-barrier (b). The induced barriers depicted in (a) have been multiplied by a factor of 40, for better visualization. All quantities shown are dimensionless.

depict snapshots of the evolving densities at several different time slices for the same scenarios of the trap displacement and quenches of the repulsion as done in 1D. In the initial two-hump ground state a dominant (99.9%) contribution comes from the $|\frac{N}{2}, \frac{N}{2}\rangle$ configuration, indicating an almost perfect twofold fragmentation. During the propagation the fragmentation changes, but the systems still remain twofold fragmented. In the upper parts of Fig. 3 we plot snapshots of the densities $|\phi_k(\mathbf{r}, t)|^2$ of the left (right) fragment $k = L, R$ and the effective time-dependent barriers $V_{jj}^{\text{eff}}(\mathbf{r}, t)$ induced by the right (left) fragment $j = R, L$.

One can clearly distinguish in Fig. 3 between the two qualitatively different regimes of evolutions: a nonviolent one, plotted in panel (b), can be contrasted with highly nonequilibrium ones, depicted in panels (a) and (c). With similar goals but substantially more effort, we have extended our investigations to the nonequilibrium many-body dynamics of a strongly repulsive trapped Bose system in 3D. The results are collected in the Supplemental Material [28], along with full movies of the respective many-body dynamics. Importantly and conclusively, we have also established the existence of these two generic regimes of many-boson evolutions in 3D setups.

Summarizing, in the nonviolent evolutions—see Figs. 2(a) and 2(b) in 1D, Fig. 3(b) in 2D, and the Supplemental Material [28] for 3D—the superposition of the interaction-induced time-dependent barriers $V_{jj}^{\text{eff}}(\mathbf{r}, t)$ and external trap $V(\mathbf{r})$ results in effective potentials which are high enough to confine the fragments also when they are moving. Hence, the physics behind the nonviolent dynamics of the trapped strongly interacting fragmented systems is indeed an under-a-barrier dynamics. Complementarily, the violent dynamics appears when the induced barriers are not high enough to trap the fragments and keep them apart from each other. In the above investigations, the heights of the induced barriers have been lowered either explicitly by the sudden decrease of the interparticle repulsion from $\lambda_0 = 0.5 \rightarrow 0.1$, or implicitly when too much internal energy was pumped into the system by the

strong $\lambda_0 = 0.5 \rightarrow 0.8$ quench leading to an increase of the energy per particle of each subcloud. In both cases the initially localized fragments start to leak out and eventually become delocalized over the entire trap.

Now, we are able to deduce a set of practical recommendations on possible experimental preparations and manipulations of trapped strongly interacting bosons. (i) Once prepared, these systems remain very stable and robust with respect to possible imperfectness of the experimental setups, because strong displacements of the traps and moderate quenches of the repulsion result in a nonviolent dynamics where the density’s “topology” and the fragmentation are preserved. (ii) A protocol where the noninteracting system is first prepared and then the interaction is diabatically quenched seems to be ineffective because it would lead to explosive dynamics. (iii) The formation of strongly interacting systems with a desired number of density humps (fragments) can be provoked and controlled by preimposing a weak optical lattice of the required periodicity before an interaction quench. By switching the lattice off afterwards, one could induce only a nonviolent dynamics.

Concluding, we have discovered two qualitatively different yet generic dynamical quantum many-body behaviors in the nonequilibrium dynamics of trapped ultracold Bose systems with strong repulsive interactions of finite range. In the first, nonviolent regime the overall “topology” of the ground-state density is preserved, whereas in the second, highly nonequilibrium explosive quantum many-body dynamics emerges. The findings have been interpreted and explained by a model in terms of interaction-induced time-dependent barriers. To shed additional light on the physics found here, further studies of many-body excitations would be instructive [43]. The generality of the discovered time-dependent physics has been verified by substantial and ample computations in one, two, and three spatial dimensions.

Computation time on the bwGRiD, HLRS, and K100 clusters is greatly acknowledged. Partial financial support by the DFG is acknowledged.

-
- [1] M. Girardeau, *J. Math. Phys.* **1**, 516 (1960).
 - [2] T. Kinoshita, T. Wenger, and D. S. Weiss, *Phys. Rev. Lett.* **95**, 190406 (2005).
 - [3] G. E. Astrakharchik and M. D. Girardeau, *Phys. Rev. B* **83**, 153303 (2011).
 - [4] F. Deuretzbacher, J. C. Cremon, and S. M. Reimann, *Phys. Rev. A* **81**, 063616 (2010).
 - [5] M. Nest, T. Klamroth, and P. Saalfrank, *J. Chem. Phys.* **122**, 124102 (2005).
 - [6] M. Nest, *Phys. Rev. A* **73**, 023613 (2006).
 - [7] J. W. Abraham, K. Balzer, D. Hochstuhl, and M. Bonitz, *Phys. Rev. B* **86**, 125112 (2012).
 - [8] Yu. E. Lozovik *et al.*, *JETP Lett.* **79**, 473 (2004).
 - [9] H. P. Büchler *et al.*, *Phys. Rev. Lett.* **98**, 060404 (2007).
 - [10] M. A. Baranov, *Phys. Rep.* **464**, 71 (2008).
 - [11] T. Lahaye, C. Menotti, L. Santos, M. Lewenstein, and T. Pfau, *Rep. Prog. Phys.* **72**, 126401 (2009).
 - [12] G. Pupillo, A. Micheli, M. Boninsegni, I. Lesanovsky, and P. Zoller, *Phys. Rev. Lett.* **104**, 223002 (2010).
 - [13] N. Henkel, F. Cinti, P. Jain, G. Pupillo, and T. Pohl, *Phys. Rev. Lett.* **108**, 265301 (2012).
 - [14] A. I. Streltsov, *Phys. Rev. A* **88**, 041602(R) (2013).
 - [15] L. Santos, G. V. Shlyapnikov, P. Zoller, and M. Lewenstein, *Phys. Rev. Lett.* **85**, 1791 (2000).
 - [16] S. Giovanazzi, P. Pedri, L. Santos, A. Griesmaier, M. Fattori, T. Koch, J. Stuhler, and T. Pfau, *Phys. Rev. A* **74**, 013621 (2006).
 - [17] Sh. Ronen, D. C. E. Bortolotti, and J. L. Bohn, *Phys. Rev. A* **74**, 013623 (2006).
 - [18] A. I. Streltsov, O. E. Alon, and L. S. Cederbaum, *Phys. Rev. Lett.* **99**, 030402 (2007).
 - [19] O. E. Alon, A. I. Streltsov, and L. S. Cederbaum, *Phys. Rev. A* **77**, 033613 (2008).
 - [20] K. Sakmann, A. I. Streltsov, O. E. Alon, and L. S. Cederbaum, *Phys. Rev. Lett.* **103**, 220601 (2009).

- [21] J. Grond, T. Betz, U. Hohenester, N. J. Mauser, J. Schmiedmayer, and T. Schumm, *New J. Phys.* **13**, 065026 (2011).
- [22] I. Březinová, A. U. J. Lode, A. I. Streltsov, O. E. Alon, L. S. Cederbaum, and J. Burgdörfer, *Phys. Rev. A* **86**, 013630 (2012).
- [23] A. U. J. Lode, K. Sakmann, O. E. Alon, L. S. Cederbaum, and A. I. Streltsov, *Phys. Rev. A* **86**, 063606 (2012).
- [24] A. U. J. Lode, A. I. Streltsov, K. Sakmann, O. E. Alon, and L. S. Cederbaum, *Proc. Natl. Acad. Sci. USA* **109**, 13521 (2012).
- [25] M. Heimsoth, D. Hochstuhl, C. E. Creffield, L. D. Carr, and F. Sols, *New J. Phys.* **15**, 103006 (2013).
- [26] H.-D. Meyer, F. Gatti, and G. A. Worth, editors, *Multidimensional Quantum Dynamics: MCTDH Theory and Applications* (Wiley-VCH, Weinheim, 2009).
- [27] N. P. Proukakis, S. A. Gardiner, M. J. Davis, and M. H. Szymanska, editors, *Quantum Gases: Finite Temperature and Non-Equilibrium Dynamics*, Vol. 1, Cold Atoms Series (Imperial College Press, London, 2013).
- [28] See Supplemental Material at <http://link.aps.org/supplemental/10.1103/PhysRevA.89.061602> for versatility of the ground states and for movies of the reported 2D and 3D MCTDHB dynamics.
- [29] O. Penrose and L. Onsager, *Phys. Rev.* **104**, 576 (1956).
- [30] P. Nozières and D. Saint James, *J. Phys. (France)* **43**, 1133 (1982).
- [31] P. Nozières, in *Bose-Einstein Condensation*, edited by A. Griffin, D. W. Snoke, and S. Stringari (Cambridge University Press, Cambridge, 1996).
- [32] R. W. Spekkens and J. E. Sipe, *Phys. Rev. A* **59**, 3868 (1999).
- [33] A. Coleman and V. Yukalov, *Reduced Density Matrices: Coulson's Challenge* (Springer, Heidelberg, 2000).
- [34] A. I. Streltsov, O. E. Alon, and L. S. Cederbaum, *Phys. Rev. A* **73**, 063626 (2006).
- [35] E. J. Mueller, T.-L. Ho, M. Ueda, and G. Baym, *Phys. Rev. A* **74**, 033612 (2006).
- [36] M. Naraschewski and R. J. Glauber, *Phys. Rev. A* **59**, 4595 (1999).
- [37] K. Sakmann, A. I. Streltsov, O. E. Alon, and L. S. Cederbaum, *Phys. Rev. A* **78**, 023615 (2008).
- [38] The effective interaction of two “dressed” atoms [40,41] reads $\tilde{W}_{dd}(|\tilde{r}_i - \tilde{r}_j|) = \frac{\Omega^4}{8\Delta^3} \frac{\hbar}{(\tilde{r}_{ij}/R_c)^{n+1}}$, where Ω is the two-photon Rabi frequency between the involved atomic levels, Δ is the detuning of the lasers with respect to the atomic transitions, and $R_c = \frac{C_n}{2\hbar|\Delta|}$ is the “screening” constant originating from the blockade phenomenon. C_n is governed by the electronic structure of the excited state; e.g., for the pure dipole-dipole (C_3/R^3) interactions $n = 3$ and for the van der Waals (C_6/R^6) – $n = 6$. In our work we use $n = 4$ corresponding to an “intermediate” situation to demonstrate the generality of the predicted physics, which holds for $n = 3$ and $n = 6$ as well. Experimental conditions reported in [42] provide the ranges R_c and interaction strength needed to observe the studied multihump fragmented states.
- [39] D. Comparat and P. Pillet, *J. Opt. Soc. Am. B* **27**, A208 (2010).
- [40] J. E. Johnson and S. L. Rolston, *Phys. Rev. A* **82**, 033412 (2010).
- [41] N. Henkel, R. Nath, and T. Pohl, *Phys. Rev. Lett.* **104**, 195302 (2010).
- [42] M. Viteau, M. G. Bason, J. Radogostowicz, N. Malossi, D. Ciampini, O. Morsch, and E. Arimondo, *Phys. Rev. Lett.* **107**, 060402 (2011).
- [43] J. Grond, A. I. Streltsov, A. U. J. Lode, K. Sakmann, L. S. Cederbaum, and O. E. Alon, *Phys. Rev. A* **88**, 023606 (2013).